

# ITERATIVE BEAM ALIGNMENT ALGORITHMS FOR TDD MIMO SYSTEMS

Dennis Ogbe, David J. Love

Purdue University  
School of Electrical and Computer Engineering  
West Lafayette, IN 47907, USA

Vasanthan Raghavan

Qualcomm, Inc.,  
Bridgewater NJ 08807, USA

## ABSTRACT

We propose two novel, low-complexity techniques for beam alignment in time division duplexing (TDD) multiple-input multiple-output (MIMO) systems. The techniques are inspired by the power method, an iterative algorithm to determine eigenvalues and eigenvectors through repeated matrix multiplications and improve upon this simple idea by providing a better performance in the low-SNR regime. The first technique sequentially constructs a least-squares estimate of the channel matrix, which is then used to calculate the optimal beamformer/combiner pair. The second technique aims to mitigate the effect of additive noise by using a linear combination of the previously tried beams to calculate the next beam in the iteration. Simulation results provide insight on the performance of both algorithms in the presence of noise and compare them with similar techniques from the literature.

**Index Terms**— Beam alignment, Beamforming, channel reciprocity, TDD, channel estimation, massive MIMO, power method.

## 1. INTRODUCTION

The two most promising multiple-input multiple-output (MIMO) applications, millimeter-wave (mmWave) MIMO [1, 2, 3, 4] and massive MIMO [5, 6, 7], rely on utilizing large beamforming gains to achieve the capacity requirements set for future 5G networks [8, 9, 10]. These gains can only be realized if sufficient channel state information (CSI) is available at the communication nodes. In traditional MIMO systems, this information is acquired by the use of channel sounding sequences and feedback [11, 12, 13, 14], which will be impractical when considering the large number of antenna elements used for mmWave and massive MIMO systems.

A common way to avoid this problem is to exploit the reciprocal nature of wireless channels using time division duplexing (TDD) systems. Channel reciprocity reduces the overall resources spent on channel sounding since CSI about the channel in one direction can be used to adapt to the channel in the reverse direction. To further reduce the amount of CSI to acquire, future systems will be forced to sound different beams during a beam alignment phase [15], eliminating the need for full CSI at the receiver and transmitter.

Many recent works such as [16, 17, 18, 19, 20, 21] have pursued a greedy TDD-based approach to obtaining good beamformers. The common theme that ties these works is the fact that repeated conjugation, normalization, and retransmission of an arbitrarily initialized beamforming vector through a reciprocal MIMO channel (with no noise) is akin to performing the power method [22] on the channel matrix. However, simple implementations like the ones pro-

posed in [16, 17, 21] are likely to perform poorly in the low-SNR regime [19]. Further work on the problem of finding good beams using the power method has been done in [19] and [23]. These techniques offer improvements on the robustness and speed of convergence of the basic power method at the cost of additional complexity. More recent approaches to the problem employ Krylov subspace methods in the context of hybrid mmWave systems [24].

Building on [19] and [23], this paper presents two novel techniques for the MIMO beam alignment problem in TDD systems with reciprocal channels. Both techniques improve on the performance of the simple power method-based algorithms, especially in low-SNR environments which are typical of practical mmWave systems. The first technique is based on the fact that a least-squares estimate of the channel matrix can be constructed sequentially using the previously used sounding beams. The channel estimates at each iteration can then be used to compute the next sounding beamformer/combiner pair, which is exchanged through a feedback link. The second technique does not require a feedback link and improves on the low-SNR performance of the basic power method by computing a normalized running sum of the previous beamformers, thus gaining greater robustness against noise through averaging. Both approaches provide useful low-complexity solutions for realizing the large beamforming gains in mmWave systems.

## 2. SYSTEM MODEL

We consider the multi-antenna communication system shown in Figure 1 consisting of two transceivers (communication nodes), with  $M_t$  antennas at node 1 and  $M_r$  antennas at node 2. The two transceivers communicate over a channel  $\mathbf{H} \in \mathbb{C}^{M_r \times M_t}$ , which we assume to be reciprocal, i.e., the channel matrix from node 1 to node 2 (uplink) is the transpose of the channel matrix from node 2 to node 1 (downlink).

Transmission on the uplink channel are precoded at node 1 by a unit-norm transmit beamforming vector  $\mathbf{f} = [f_1 \ f_2 \ \dots \ f_{M_t}]^T \in \mathbb{C}^{M_t}$ , sent over the channel, and combined at node 2 with a unit-norm receive combiner  $\mathbf{z} = [z_1 \ z_2 \ \dots \ z_{M_r}]^T \in \mathbb{C}^{M_r}$ . A data symbol  $s_o[\ell]$  sent on the uplink channel thus results in the received symbol

$$r_o[\ell] = \sqrt{\rho_o} \mathbf{z}^* \mathbf{H} \mathbf{f} s_o[\ell] + n_o[\ell], \quad (1)$$

where  $\rho_o$  is the uplink signal-to-noise ratio (SNR),  $n_o[\ell] \sim \mathcal{CN}(0, 1)$  is a complex additive white Gaussian noise sample, and  $(\cdot)^*$  denotes complex transposition. Similarly, for a data symbol  $s_e[\ell]$  sent on the downlink channel, node 1 obtains the received symbol

$$r_e[\ell] = \sqrt{\rho_e} \mathbf{f}^T \mathbf{H}^T \bar{\mathbf{z}} s_e[\ell] + n_e[\ell], \quad (2)$$

where  $\bar{\cdot}$  denotes complex conjugation.

This material is based upon work supported in part by the National Science Foundation under Grant No. CNS-1642982.

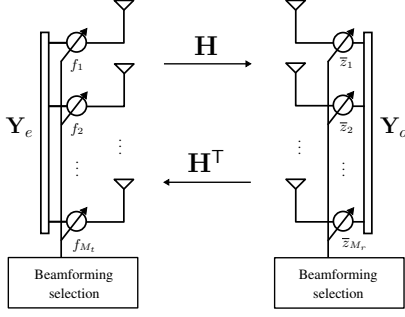


**Fig. 1.** Communication node 1 transmits data over the uplink channel  $\mathbf{H}$  with node 2, while node 2 transmits data over the downlink channel  $\mathbf{H}^T$ . The nodes precode and combine their transmitted and received signals using the beamforming vectors  $\mathbf{f}$  and  $\mathbf{z}$

The terms  $|\mathbf{z}^* \mathbf{H} \mathbf{f}|^2 = |\mathbf{f}^T \mathbf{H}^T \mathbf{z}|^2$  represent the effective channel gain, which we want to maximize in order to achieve reliable communications and the highest possible data rate in both directions. We denote the beams that achieve this as  $\mathbf{f}_{\text{opt}}$  and  $\mathbf{z}_{\text{opt}}$ . It is well-known from [25, 26] that the effective channel gain is maximized when  $\mathbf{f}$  and  $\mathbf{z}$  are the right and left singular vectors of  $\mathbf{H}$  corresponding to the largest singular value of  $\mathbf{H}$  and that its maximum achievable value is  $\|\mathbf{H}\|_2^2 = \lambda_{\max}(\mathbf{H}^* \mathbf{H})$ . Furthermore, we assume that neither transceiver has knowledge of the channel, rendering it impossible for either node to compute the estimates of  $\mathbf{f}_{\text{opt}}$  and  $\mathbf{z}_{\text{opt}}$  using the singular value decomposition (SVD). Instead, as mentioned earlier, these estimates are obtained iteratively during a beam alignment phase.

In the proposed techniques, both nodes cooperatively determine  $\mathbf{f}_{\text{opt}}$  and  $\mathbf{z}_{\text{opt}}$  during the beam alignment phase by exploiting the channel's reciprocity property. To model this, our system operates on a *ping-pong* observation framework, which divides each discrete channel use into two time slots [15]. During slot 1 (*ping*), node 1 transmits training data to node 2 on the uplink channel  $\mathbf{H}$ . During slot 2 (*pong*), node 2 transmits training data back to node 1 on the downlink channel  $\mathbf{H}^T$ . Since the training data is irrelevant to the beamforming weights, we restrict our attention to the transmit and receive beam during the  $k$ -th ping-pong period, which, for slot 1, is given as

$$\mathbf{y}_o[k] = \sqrt{\rho_o} \mathbf{H} \mathbf{f}[k] + \mathbf{n}_o[k]. \quad (3)$$

In (3), the term  $\mathbf{f}[k]$  denotes an estimate of  $\mathbf{f}_{\text{opt}}$  at training phase time-index  $k$  and  $\mathbf{n}_o[k] \sim \mathcal{CN}(\mathbf{0}, \mathbf{I})$  is a complex Gaussian noise vector of size  $M_r$ . Due to the reciprocity of the uplink and downlink channels, the observation at slot 2 is given as

$$\mathbf{y}_e[k] = \sqrt{\rho_e} \mathbf{H}^T \mathbf{z}[k] + \mathbf{n}_e[k]. \quad (4)$$

Similar to (3),  $\rho_e$  denotes the downlink training SNR,  $\mathbf{z}[k]$  denotes the estimate of  $\mathbf{z}_{\text{opt}}$  at training phase time-index  $k$  and  $\mathbf{n}_e[k] \sim \mathcal{CN}(\mathbf{0}, \mathbf{I})$  is a complex Gaussian noise vector of size  $M_t$ .

### 3. SEQUENTIAL LEAST SQUARES (SLS) POWER METHOD

In the first scheme, each transceiver sequentially constructs a least-squares estimate of  $\mathbf{H}$  before each ping-pong time slot, which is then used to compute the next state of its beamforming vector. This computation of the beamforming vector follows directly from the

SVD theorem [22], which states that we can obtain the left singular vector of a matrix  $\mathbf{A} = \mathbf{U} \mathbf{\Sigma} \mathbf{V}^*$  by multiplying  $\mathbf{A}$  with its right singular vector and vice versa.

Since the channel matrix is unknown at either side of the communication link, the transceivers construct an estimate of it before each time slot. These estimates are constructed using all of the previous estimates of  $\mathbf{f}_{\text{opt}}$  and  $\mathbf{z}_{\text{opt}}$ . In particular, using all beamforming vectors upto time slot  $k$ , we can write (3) and (4) in matrix form as

$$\mathbf{Y}_{o,k} = \sqrt{\rho_o} \mathbf{H} \mathbf{F}_k + \mathbf{N}_{o,k} \quad (5)$$

and

$$\mathbf{Y}_{e,k} = \sqrt{\rho_e} \mathbf{H}^T \mathbf{Z}_k + \mathbf{N}_{e,k}. \quad (6)$$

In eqns. (5) and (6),  $\mathbf{F}_k = [\mathbf{f}[0] \ \mathbf{f}[1] \ \dots \ \mathbf{f}[k]]$  and  $\mathbf{Z}_k = [\mathbf{z}[0] \ \mathbf{z}[1] \ \dots \ \mathbf{z}[k]]$  contain all of the estimates of  $\mathbf{f}_{\text{opt}}$  and  $\mathbf{z}_{\text{opt}}$  up to ping-pong period  $k$ . Furthermore, note that the matrices  $\mathbf{Y}_{o,k} = [\mathbf{y}_o[0] \ \mathbf{y}_o[1] \ \dots \ \mathbf{y}_o[k]]$  and similarly  $\mathbf{Y}_{e,k} = [\mathbf{y}_e[0] \ \mathbf{y}_e[1] \ \dots \ \mathbf{y}_e[k]]$  contain all of the observed signal vectors, respectively.

Based on this information, transceiver 1 constructs an estimate of the channel by solving the least-squares problem

$$\hat{\mathbf{H}}_{e,k} = \underset{\tilde{\mathbf{H}} \in \mathbb{C}^{M_r \times M_t}}{\text{argmin}} \left( \left\| \mathbf{Y}_{e,k-1}^T - \sqrt{\rho_e} \tilde{\mathbf{H}} \mathbf{F}_{k-1} \right\|_F^2 \right). \quad (7)$$

Similarly, transceiver 2 constructs an estimate of the channel by solving

$$\hat{\mathbf{H}}_{o,k} = \underset{\tilde{\mathbf{H}} \in \mathbb{C}^{M_r \times M_t}}{\text{argmin}} \left( \left\| \mathbf{Y}_{o,k} - \sqrt{\rho_o} \tilde{\mathbf{H}} \mathbf{F}_k \right\|_F^2 \right). \quad (8)$$

Note that there exists an asymmetry in the time-index between (7) and (8). The solutions to these least-squares problems ( $\hat{\mathbf{H}}_{e,k}$  and  $\hat{\mathbf{H}}_{o,k}$ ) can be obtained using the Moore-Penrose pseudoinverse, which we call the *batch* approach. Clearly, the estimation error is monotonically decreasing in the SNRs,  $\rho_o$  and  $\rho_e$ . Once  $\hat{\mathbf{H}}_{e,k}$  has been estimated, applying the SVD theorem, we note that the nodes can compute estimates of their optimal beamformers  $\mathbf{f}_{\text{opt}}$  and  $\mathbf{z}_{\text{opt}}$  as

$$\hat{\mathbf{f}}[k] = \frac{\hat{\mathbf{H}}_{e,k}^* \mathbf{z}[k-1]}{\left\| \hat{\mathbf{H}}_{e,k}^* \mathbf{z}[k-1] \right\|_2}, \quad \hat{\mathbf{z}}[k] = \frac{\hat{\mathbf{H}}_{o,k} \mathbf{f}[k]}{\left\| \hat{\mathbf{H}}_{o,k} \mathbf{f}[k] \right\|_2}. \quad (9)$$

The batch least-squares estimators are traditionally obtained by computing the Moore-Penrose pseudoinverse using the SVD. For large  $k$ , this can become computationally intensive. Our method therefore uses a sequential algorithm [27] that updates each previous channel estimate based on the current received signal vector. This approach minimizes computational burden as well as eliminates the need to store all of the previous received signal vectors and beamforming vectors.

Since (9) uses the conjugate transpose of the channel to compute a new beamformer, we can use an algorithm that directly computes an estimate for the conjugate transpose of the channel,  $\hat{\mathbf{H}}_{e,k}^*$ . This choice is made here simply to make the derivation of the sequential formulas more consistent between the two nodes. In this setup, the sequential solution to of (8) (the channel estimator update) is given as

$$\hat{\mathbf{H}}_{e,k}^* = \hat{\mathbf{H}}_{e,k-1}^* + \left( \frac{\bar{\mathbf{y}}_e[k-1]}{\sqrt{\rho_e}} - \hat{\mathbf{H}}_{e,k-1}^* \mathbf{z}[k-1] \right) \mathbf{K}_{e,k} \quad (10)$$

where

$$\mathbf{K}_{e,k} = \frac{\mathbf{z}^*[k-1]\mathbf{C}_{e,k-1}}{1 + \mathbf{z}^*[k-1]\mathbf{C}_{e,k-1}\mathbf{z}[k-1]} \quad (11)$$

and the covariance matrix update is given as

$$\mathbf{C}_{e,k} = \mathbf{C}_{e,k-1} (\mathbf{I} - \mathbf{z}[k-1]\mathbf{K}_{e,k}). \quad (12)$$

After obtaining  $\widehat{\mathbf{H}}_{e,k}^*$ , node 1 uses (9) to obtain the  $k$ -th estimate for  $\mathbf{f}_{\text{opt}}$ . The value of this beamformer then needs to be fed back to node 2, where it will be used to obtain the next estimate for  $\mathbf{z}_{\text{opt}}$ . At node 2, the same sequential algorithm is used to solve the least-squares problem, and the update expression for  $\widehat{\mathbf{H}}_{o,k}$  becomes

$$\widehat{\mathbf{H}}_{o,k} = \widehat{\mathbf{H}}_{o,k-1} + \left( \frac{\mathbf{y}_o[k]}{\sqrt{\rho_o}} - \widehat{\mathbf{H}}_{o,k-1}\mathbf{f}[k] \right) \mathbf{K}_{o,k} \quad (13)$$

where

$$\mathbf{K}_{o,k} = \frac{\mathbf{f}^*[k]\mathbf{C}_{o,k-1}}{1 + \mathbf{f}^*[k]\mathbf{C}_{o,k-1}\mathbf{f}[k]} \quad (14)$$

with the covariance matrix update

$$\mathbf{C}_{o,k} = \mathbf{C}_{o,k-1} (\mathbf{I} - \mathbf{f}[k]\mathbf{K}_{o,k}). \quad (15)$$

Node 2 then obtains  $\mathbf{z}[k]$  from (9), which in turn is fed back to node 1. We note that the feedback requirements, which are on the order of the number of antenna elements in the system, are small given the multi-Gbps rates expected from mmWave and massive MIMO systems and thus do not reduce the practicality of this approach, especially given its performance in low-SNR environments.

We observe that these sequential least-squares estimators are only equivalent to their batch estimators when the beamformer matrices  $\mathbf{F}_k$  and  $\mathbf{Z}_k$  are of full column rank. That is, for  $k < \text{rank}[\mathbf{H}]$ , both nodes would need to compute their channel estimates using the batch approach. Hence, we propose to initialize  $\mathbf{f}[-1]$  and  $\mathbf{z}[-1]$  with complex random unit-norm vectors. We then use the batch estimators for  $k < \text{rank}[\mathbf{H}]$  and switch to the sequential estimators after the iteration  $k = \text{rank}[\mathbf{H}]$ . As the channel estimates converge to the true channel with the number of iterations, the steps outlined in (9) essentially perform a two-iteration power method without noise, which converges at a rate of  $(\sigma_1/\sigma_2)^2$  [22].

For large channel matrices, it can be computationally difficult to use the batch estimator for the first  $M_t$  iterations. In this case, it can be shown analytically and it has been verified in Section 5 that the SLS power method delivers sufficient performance when using the sequential estimators starting with the first iteration. In this setup, the nodes initialize  $\mathbf{f}[-1]$  and  $\mathbf{z}[-1]$  with complex random unit-norm vectors and transmit these vectors across  $\mathbf{H}$  according to (3) and (4) and compute their initial rank-1 channel estimates using the Moore-Penrose pseudoinverse, which reduces to a conjugate transposition, since  $\mathbf{F}_k$  and  $\mathbf{Z}_k$  both have only one column when  $k = 0$ . To ensure convergence of the channel estimates to the true channels, the nodes then initialize  $\mathbf{C}_{o,-1}$  and  $\mathbf{C}_{e,-1}$  to  $\alpha\mathbf{I}$ , where  $\alpha$  is a large real number [28] and use the sequential formulas (10)-(15) to estimate their beamformers.

#### 4. SUMMED POWER METHOD

In the second scheme, both transceivers calculate their next beamformers based on a normalized running sum of their previous observations. The transceivers do not need a feedback link, as neither

transceiver needs to have knowledge of the other transceiver's beamformer. For notational convenience, we consider a square channel matrix in this section. Without loss in generality, we can transform an  $M_t \times M_r$  channel matrix to an  $M \times M$  channel matrix by appending zero columns/rows until we arrive at a square matrix. Then, as described in Section 2, both nodes exchange training symbols according to (3) and (4). However, instead of simply conjugating and retransmitting their received vector as in the simple power method, both nodes obtain their next beamformers from a running sum of all of their previous received vectors. During the  $k$ -th ping-pong period, node 1 computes its next beamformer as

$$\begin{aligned} \mathbf{f}[k] &= \alpha_{k-1} [\bar{\mathbf{y}}_e[k-1] + \bar{\mathbf{y}}_e[k-2] + \dots + \bar{\mathbf{y}}_e[1]] \\ &= \alpha_{k-1} \mathbf{s}_e[k-1]. \end{aligned} \quad (16)$$

Similarly, node 2 computes its next beamformer as

$$\begin{aligned} \mathbf{z}[k] &= \beta_{k-1} [\mathbf{y}_o[k-1] + \mathbf{y}_o[k-2] + \dots + \mathbf{y}_o[1]] \\ &= \beta_{k-1} \mathbf{s}_o[k-1]. \end{aligned} \quad (17)$$

In the above equations,  $\mathbf{s}_e[k]$  and  $\mathbf{s}_o[k]$  are the state vectors at each node which hold the running sum of the received vectors. The terms  $\alpha_k = 1/\|\mathbf{s}_e[k]\|_2$  and  $\beta_k = 1/\|\mathbf{s}_o[k]\|_2$  are normalization terms to impose a unit-norm power constraint.

The main idea behind this technique is to average out noisy estimates of the singular vector estimates  $\mathbf{f}[k]$  and  $\mathbf{z}[k]$  during each ping-pong period. Convergence properties are notoriously difficult to prove when considering general channel matrices, but it is possible for some special cases. We will thus consider diagonal channel matrices with ordered elements on the diagonal for the remainder of this paper. This can equivalently be thought of as performing all of the signal processing within the bases corresponding to the left and right singular vectors of the true channel. As we will show in Section 5, our simulation results indicate that the algorithm converges for general channel matrices as well. With the above assumptions, we can then write the  $2M$ -dimensional state vector  $\mathbf{s}[k]$  for both nodes as

$$\begin{aligned} \mathbf{s}[k] &= \begin{bmatrix} \mathbf{s}_e[k] \\ \mathbf{s}_o[k] \end{bmatrix} = \begin{bmatrix} \mathbf{I} & \sqrt{\rho_e} \beta_{k-1} \mathbf{H}^* \\ \sqrt{\rho_o} \alpha_{k-1} \mathbf{H} & \mathbf{I} \end{bmatrix} \mathbf{s}[k-1] + \mathbf{n}[k] \\ &= \prod_{i=0}^{k-1} \begin{bmatrix} \mathbf{I} & \sqrt{\rho_e} \beta_{k-1-i} \mathbf{H}^* \\ \sqrt{\rho_o} \alpha_{k-1-i} \mathbf{H} & \mathbf{I} \end{bmatrix} \mathbf{s}[0] \\ &\quad + \sum_{\ell=1}^k \prod_{j=\ell}^{k-1} \begin{bmatrix} \mathbf{I} & \sqrt{\rho_e} \beta_{k-1+\ell-j} \mathbf{H}^* \\ \sqrt{\rho_o} \alpha_{k-1+\ell-j} \mathbf{H} & \mathbf{I} \end{bmatrix} \mathbf{n}[\ell] \end{aligned} \quad (18)$$

Since the optimal beamformers in this setup are scalar multiples of the first column of the  $M \times M$  identity matrix, it is now our objective to show that the combined state vector  $\mathbf{s}[k]$  approaches the vector  $\mathbf{s}_{\text{opt}} = [\alpha \ 0 \ \dots \ 0 \ \beta \ 0 \ \dots \ 0]^T$  for some  $\alpha$  and  $\beta$  as the number of iterations  $k$  grows large. The optimal beamformers are defined only up to a point on the Grassmannian manifold, which explains the impreciseness in the factors  $\alpha$  and  $\beta$ . It is shown in [28] that for the given assumptions, the normalizing factors  $\alpha_k$  and  $\beta_k$  are approximately equal. Using this fact, we can observe that the state transition matrix from (18) is diagonalized by the unitary matrix

$$\tilde{\mathbf{U}} = \frac{1}{\sqrt{2}} \begin{bmatrix} \mathbf{I} & \mathbf{I} \\ \mathbf{I} & -\mathbf{I} \end{bmatrix}. \quad (19)$$

It can further be shown that the state-space model from (18) can then be rewritten as

$$\begin{aligned} \mathbf{s}[k] &= \tilde{\mathbf{U}} \left[ \prod_{i=0}^{k-1} \begin{pmatrix} \mathbf{I} + \sqrt{\rho} \alpha_i \mathbf{H} & \mathbf{0} \\ \mathbf{0} & \prod_{i=0}^{k-1} (\mathbf{I} - \sqrt{\rho} \alpha_i \mathbf{H}) \end{pmatrix} \right] \tilde{\mathbf{U}}^* \mathbf{s}[0] \\ &+ \tilde{\mathbf{U}} \sum_{\ell=1}^k \left[ \prod_{j=\ell}^{k-1} \begin{pmatrix} \mathbf{I} + \sqrt{\rho} \alpha_j \mathbf{H} & \mathbf{0} \\ \mathbf{0} & \prod_{j=\ell}^{k-1} (\mathbf{I} - \sqrt{\rho} \alpha_j \mathbf{H}) \end{pmatrix} \right] \tilde{\mathbf{U}}^* \mathbf{n}[\ell], \end{aligned} \quad (20)$$

where we have made the further simplification of assuming  $\rho_o = \rho_e = \rho$  to simplify the analysis. Using this observation, the results of Theorem 1 can be obtained.

**Theorem 1.**  $\mathbf{s}[k] \rightarrow \mathbf{s}_{\text{opt}}$  as  $k$  increases.

For the full proof, see Section IV of [28]. The outline of the proof is as follows. We focus on the diagonal matrices  $\tilde{\mathbf{\Lambda}}_{k-1,\ell}$ , obtained by diagonalizing the state-space model of (20). They are given as

$$\tilde{\mathbf{\Lambda}}_{k-1,\ell} = \left[ \prod_{i=\ell}^{k-1} \begin{pmatrix} \mathbf{I} + \sqrt{\rho} \alpha_i \mathbf{H} & \mathbf{0} \\ \mathbf{0} & \prod_{i=\ell}^{k-1} (\mathbf{I} - \sqrt{\rho} \alpha_i \mathbf{H}) \end{pmatrix} \right]. \quad (21)$$

It can then be shown that the diagonal entries of  $\tilde{\mathbf{\Lambda}}_{k-1,\ell}$  are dominated by first and the  $(M-1)$ -th entry. The repeated multiplication and normalization steps then ensure that the first and the  $(M-1)$ -th entry of  $\mathbf{s}[k]$  dominate over the others, converging to a vector of the form  $[\alpha \ 0 \ \dots \ 0 \ \beta \ 0 \ \dots \ 0]^T$  for some  $\alpha$  and  $\beta$ .

## 5. SIMULATION RESULTS

Figures 2 and 3 compare the performance of our proposed algorithms to the techniques presented in [16] and [19] using Monte-Carlo methods. Since we are only interested in the dominant singular vectors, we used the one-dimensional versions of the algorithms. The value of the design parameter  $\mu$  for the BSM algorithm from [19] was  $1.5k$  in each of the simulations. The SLS power method curve uses the sequential estimator starting at the first iteration after properly initializing the covariance matrices  $\mathbf{C}_{o,-1}$  and  $\mathbf{C}_{e,-1}$  as outlined in Section 3. The figures show the results for uplink and downlink SNRs of 0 dB (solid lines) and 20 dB (dashed lines). We consider two performance metrics: i) instantaneous effective channel gain  $|\mathbf{z}^*[k] \mathbf{H} \mathbf{f}[k]|^2$  at time index  $k$ , and ii) the angle between the true singular vector  $\mathbf{f}_{\text{opt}}$  and its estimate  $\mathbf{f}[k]$ , given as  $\phi_k = \cos^{-1}(|\mathbf{f}_{\text{opt}}^* \mathbf{f}[k]|)$ .

We also note that in order to average results over different channel realizations, we normalize the values of the effective channel gain by the ideal channel gain with full CSI at the receiver and transmitter, which is equal to the matrix 2-norm of the channel. Fast convergence of the algorithm then means fast convergence of the normalized instantaneous effective channel gain to 1. In all cases, the SLS power method yields the fastest and most accurate results. At high SNR values, the BIMA algorithm from [16] performs on par with the SLS method and is the better choice due to its low computational complexity. The situation is different at a low SNR. Here, the BIMA is clearly inferior to the other algorithms, while the SLS method still delivers good performance. The strength of the summed power method is evident in the low-SNR curves, where it produces desirable results despite very low computational overhead with respect to the BIMA algorithm. The results indicate that the

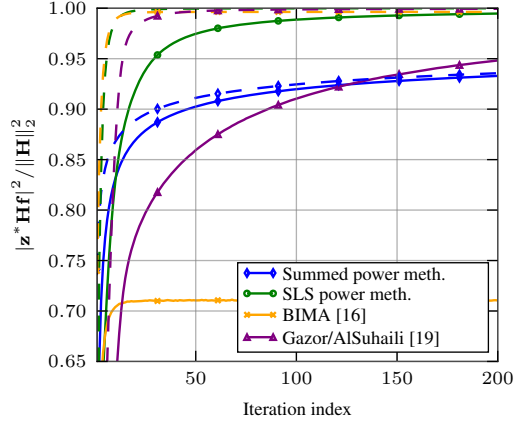


**Fig. 2.** Average values of the effective channel gain  $|\mathbf{z}^* \mathbf{H} \mathbf{f}|^2$ , normalized by the ideal CSI gain  $\|\mathbf{H}\|_2^2$  for a  $32 \times 4$  MIMO system. Solid lines: 0 dB SNR. Dashed lines: 20 dB SNR. Averaged over 60000 runs.

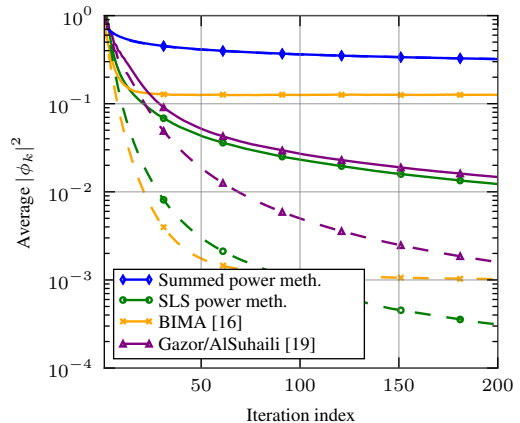


**Fig. 3.** Average of the square of the difference angle  $\phi$  between  $\mathbf{f}_{\text{opt}}$  and its estimate  $\mathbf{f}[k]$  for a  $32 \times 4$  MIMO system. Solid lines: 0 dB SNR. Dashed lines: 20 dB SNR. Averaged over 60000 runs.

SLS power method should be the preferred choice for systems without constraints in computational complexity. If the computational overhead of the SLS power method is too high, a combination of the BIMA algorithm and the summed power method seems to be a good choice. In this setup, the BIMA algorithm would be used in the high SNR regime, while the summed power method would be used in low SNRs. The combination of both techniques does not increase the complexity of the implementation, since both algorithms are very similar.

## 6. CONCLUSION

We studied the problem of estimating the dominant singular vectors of a MIMO channel matrix in a low-SNR environment. We presented two novel approaches to address this problem, both delivering improved performance compared to prior work. We presented the convergence behavior of both approaches through analysis and numerical studies.

## 7. REFERENCES

- [1] F. Khan and Z. Pi, "An introduction to millimeter wave mobile broadband systems," *IEEE Commun. Magaz.*, vol. 49, no. 6, pp. 101–107, June 2011.
- [2] T. S. Rappaport, S. Sun, R. Mayzus, H. Zhao, Y. Azar, K. Wang, G. N. Wong, J. K. Schulz, M. Samimi, and F. Gutierrez, "Millimeter wave mobile communications for 5G cellular: It will work!," *IEEE Access*, vol. 1, pp. 335–349, 2013.
- [3] S. Rangan, T. S. Rappaport, and E. Erkip, "Millimeter-wave cellular wireless networks: Potentials and challenges," *Proc. IEEE*, vol. 102, no. 3, pp. 366–385, Mar. 2014.
- [4] A. L. Swindlehurst, E. Ayanoglu, P. Heydari, and F. Capolino, "Millimeter-wave massive MIMO: The next wireless revolution?," *IEEE Commun. Magaz.*, vol. 52, no. 9, pp. 56–62, Sept. 2014.
- [5] T. L. Marzetta, "Non-cooperative cellular wireless with unlimited numbers of base station antennas," *IEEE Trans. Wireless Commun.*, vol. 9, no. 11, pp. 3590–3600, Nov. 2010.
- [6] H. Q. Ngo, E. G. Larsson, and T. L. Marzetta, "Energy and spectral efficiency of very large multiuser MIMO systems," *IEEE Trans. Commun.*, vol. 61, no. 4, pp. 1436–1449, Apr. 2013.
- [7] F. Rusek, D. Persson, B. K. Lau, E. G. Larsson, T. L. Marzetta, O. Edfors, and F. Tufvesson, "Scaling up MIMO: Opportunities and challenges with very large arrays," *IEEE Sig. Proc. Magaz.*, vol. 30, no. 1, pp. 40–60, Jan. 2013.
- [8] Aalto University, AT&T, BUP, CMCC, Ericsson, Huawei, Intel, KT Corporation, Nokia, NTT DOCOMO, NYU, Qualcomm, Samsung, U. Bristol, and USC, "White paper on '5G Channel Model for bands up to 100 GHz'," v2.3, Oct. 2016.
- [9] D. Gesbert, M. Kountouris, R. W. Heath, Jr., C.-B. Chae, and T. Salzer, "Shifting the MIMO paradigm: From single user to multiuser communications," *IEEE Sig. Proc. Magaz.*, vol. 24, no. 5, pp. 36–46, Oct. 2007.
- [10] Q. H. Spencer, C. B. Peel, A. L. Swindlehurst, and M. Haardt, "An introduction to the multi-user MIMO downlink," *IEEE Commun. Magaz.*, vol. 42, no. 10, pp. 60–67, Oct. 2004.
- [11] D. J. Love, R. W. Heath, Jr., and T. Strohmer, "Grassmannian beamforming for multiple-input multiple-output wireless systems," *IEEE Trans. Inform. Theory*, vol. 49, no. 10, pp. 2735–2747, Oct. 2003.
- [12] K. K. Mukkavilli, A. Sabharwal, E. Erkip, and B. Aazhang, "On beamforming with finite rate feedback in multiple-antenna systems," *IEEE Trans. Inform. Theory*, vol. 49, no. 10, pp. 2562–2579, Oct. 2003.
- [13] F. Boccardi, B. Clerckx, A. Ghosh, E. Hardouin, G. Jöngren, K. Kusume, E. Onggosanusi, and Y. Tang, "Multiple antenna techniques in LTE-Advanced," *IEEE Commun. Magaz.*, vol. 50, no. 2, pp. 114–121, Mar. 2012.
- [14] C. Lim, T. Yoo, B. Clerckx, B. Lee, and B. Shim, "Recent trend of multiuser MIMO in LTE-Advanced," *IEEE Commun. Magaz.*, vol. 51, no. 3, pp. 127–135, Mar. 2013.
- [15] S. Hur, T. Kim, D. J. Love, J. V. Krogmeier, T. A. Thomas, and A. Ghosh, "Millimeter wave beamforming for wireless backhaul and access in small cell networks," *IEEE Trans. Commun.*, vol. 61, no. 10, pp. 4391–4403, Oct. 2013.
- [16] T. Dahl, N. Christophersen, and D. Gesbert, "Blind MIMO eigenmode transmission based on the algebraic power method," *IEEE Trans. Sig. Proc.*, vol. 52, no. 9, pp. 2424–2431, Sept. 2004.
- [17] Y. Tang, B. Vucetic, and Y. Li, "An iterative singular vectors estimation scheme for beamforming transmission and detection in MIMO systems," *IEEE Commun. Letters*, vol. 9, no. 6, pp. 505–507, June 2005.
- [18] S. Mandelli and M. Magarini, "Blind iterative singular vectors estimation and adaptive spatial loading in a reciprocal MIMO channel," *Proc. IEEE Wireless Commun. and Netwk. Conf., Istanbul, Turkey*, pp. 1036–1041, Apr. 2014.
- [19] S. Gazor and K. AlSuhaili, "Communications over the best singular mode of a reciprocal MIMO channel," *IEEE Trans. Commun.*, vol. 58, no. 7, pp. 1993–2001, July 2010.
- [20] T. Dahl, S. S. Pereira, N. Christophersen, and D. Gesbert, "Intrinsic subspace convergence in TDD MIMO communication," *IEEE Trans. Sig. Proc.*, vol. 55, no. 6, pp. 2676–2687, June 2007.
- [21] V. Raghavan, J. Cezanne, S. Subramanian, A. Sampath, and O. H. Koymen, "Beamforming tradeoffs for initial UE discovery in millimeter-wave MIMO systems," *IEEE Journ. Sel. Topics in Sig. Proc.*, vol. 10, no. 3, pp. 543–559, Apr. 2016.
- [22] G. H. Golub and C. F. Van Loan, *Matrix Computations*, Johns Hopkins University Press, Baltimore, fourth edition, Dec. 2012.
- [23] R. Prasad, B. N. Bharath, and C. R. Murthy, "Joint data detection and dominant singular mode estimation in time varying reciprocal MIMO systems," *Proc. IEEE Intern. Conf. on Acoust., Speech and Sig. Proc., Prague, Czech Rep.*, pp. 3240–3243, May 2011.
- [24] H. Ghauch, T. Kim, M. Skoglund, and M. Bengtsson, "Subspace Estimation and Decomposition in large millimeter-wave MIMO systems," *IEEE Journ. Sel. Topics in Sig. Proc.*, vol. 10, no. 3, pp. 528–542, Apr. 2016.
- [25] D. J. Love and R. W. Heath, Jr., "Equal gain transmission in multiple-input multiple-output wireless systems," *IEEE Trans. Commun.*, vol. 51, no. 7, pp. 1102–1110, July 2003.
- [26] C.-H. Tse, K.-W. Yip, and T.-S. Ng, "Performance tradeoffs between maximum ratio transmission and switched-transmit diversity," *Proc. IEEE Intern. Symp. Pers. Indoor and Mob. Radio Commun., London, UK*, vol. 2, pp. 1485–1489, Sept. 2000.
- [27] S. Kay, *Fundamentals of Statistical Signal Processing, Volume I: Estimation Theory*, Prentice Hall, Englewood Cliffs, N.J., 1st edition, Apr. 1993.
- [28] D. Ogbe, D. J. Love, and V. Raghavan, "Noisy Beam Alignment Techniques for Reciprocal MIMO Channels," *arXiv:1609.03601 [cs.IT]*, Nov. 2016.